Hindawi
Advances in Civil Engineering
Volume 2022, Article ID 2011786, 11 pages
https://doi.org/10.1155/2022/2011786

Research Article

Compression Performance and Calculation Method of Thin-Walled Prefabricated Steel Tube Lightweight Concrete Columns

Yue Li[1], **Xinlan Wu**[1], **Xiaorun Li**[2], **Kechao Zhang**[3], **and Chongming Gao**[4]

[1]*School of Civil Engineering, North China University of Technology, Beijing 100144, China*
[2]*Central Research Institute of Building and Construction Co., Ltd., MCC Group, Beijing 100088, China*
[3]*Research Institute of Highway Ministry of Transport, Beijing 100088, China*
[4]*The Key Laboratory of Urban Security and Disaster Engineering, Ministry of Education, Beijing University of Technology, Beijing 100124, China*

Correspondence should be addressed to Xiaorun Li; 676897984@qq.com

Received 17 March 2022; Revised 2 June 2022; Accepted 27 June 2022; Published 12 August 2022

Academic Editor: Cong Zhang

To investigate the axial compression performance of cold-formed thin-walled steel tube lightweight concrete columns, the compressive test was carried out on four groups of 12 specimens. And the effects of factors such as section size, concrete strength, and steel content of the members on the axial compression bearing capacity were investigated. The results show that (1) the main failure of the cold-formed thin-walled steel lightweight concrete column is the local buckling of the steel wall and crushed of the core concrete. The presence of infill concrete suppressed and delayed the buckling of the tube wall. (2) The bearing capacity of cold-formed thin-walled steel lightweight concrete columns increases with the strength of the infill concrete. When the slenderness ratio is same, the bearing capacity and ductility of the columns with more steel content are higher than those of lower steel content. (3) The calculation method of the bearing capacity for the cold-formed thin-walled steel lightweight concrete column was proposed and verified.

1. Introduction

The cold-formed thin-walled steel tube has the advantages of light weight and easy installation. Due to the thin wall thickness of the tube, the member is greatly affected by initial defects and prone to local buckling instability [1]. Light aggregate concrete has the advantages of light self-weight and good thermal insulation performance but low strength and poor plasticity. Therefore, by combining the advantages of the materials, the cold-formed thin-walled steel tube lightweight concrete columns are increasingly used in buildings, bridges engineering, etc. [2].

At present, the buckling capacity of the thin-walled steel structures is topical issues. Yao and Wu [3] studied the influence of distortion defects on the mechanical properties of cold-formed thin-walled steel columns and found that the initial defect had a great impact on the ultimate bearing capacity of the specimen. Whittle and Ramseyer [4] conducted a compressive experimental investigation of cold-formed, built-up C-channels columns and got the relationship of the axial buckling capacity and the slenderness ratio. Zhou and Yang [5] conducted the axial compressive experiment on the four limbs cold-formed thin-walled steel columns, which found that the ultimate bearing capacity was significantly improved by reducing the flange width-to-thickness ratio of the column section. Li et al. [6] investigated the axial compressive capacity of cold-formed thin-walled steel columns with double channel sections and analyzed the influence of installation error and connector spacing on the bearing capacity. Nie and Huo [7, 8] conducted eccentric compressive experiments on the four limbs and double-limb built-up cold-formed thin-walled box-section columns and found that the ultimate bearing capacity and stiffness were decreased with the increase of the slenderness ratio and the eccentricity. Zhou and Guan [9] analyzed the bending performance of double-limb cold-formed thin-walled I-section beams and proposed the strength reduction correction method for the flexural bearing capacity of the beams with web openings and two limbs. Moen and Schafer [10] studied the cold-formed steel columns with holes and the results showed that slotted web holes had a minimal influence on the ultimate strength of the specimens. In terms of the design method, Chen [11] studied the stub column tests of thin-walled complex section with intermediate stiffeners and found that the design strengths calculated by the direct strength method are based on the buckling stresses obtained from finite element analysis results generally agreed with the test results. Young and Chen [12] studied the design of cold-formed steel built-up closed sections with intermediate stiffeners and showed that the direct strength method using a single section to obtain the buckling stresses was generally conservative.

However, there are few studies on cold-formed thin-walled steel tube lightweight concrete structures. Uy [13] studied the buckling mode of thin-walled steel pipe concrete columns and the buckling performance to determine the slenderness limit. Pricher et al. [14] proposed an improved design method for the effect of initial defects in the fabrication of thin-walled square steel tube concrete specimens on the load bearing capacity. An and Han [15] studied the performance of concrete-encased thin-walled steel tube columns under combined compression and bending and analyzed the influence of material strength, steel ratio et al. on the sectional capacity of the columns. Han et al. [16] studied the behavior of high-strength concrete filled cold-formed steel tubes under transverse impact loading.

As the demand continues to rise, the efficient and accurate design of for cold-formed thin-walled steel lightweight concrete structures is essential. One frequently used cold-formed steel member is a built-up member, formed by two or more attached steel elements. Since the inner concrete helps to suppress buckling of the thin-walled tube, a novel section of the cold-formed thin-walled steel lightweight concrete column was proposed. And the axial performance of the columns was studied by a compressive test. The results can be referred by the practical design and specifications for the similar structure.

2. Axial Compression Test

2.1. Specimens Design. The production process of the specimen is shown in Figure 1. The specimens were made of Q345 weathering steel which was first processed into C-shape. Then the other steel plate was connected with the C-shape steel by ST4.8 self-tapping nails to form a closed rectangle section. Spherical shale ceramic granules and expanded perlite granules were selected as the coarse and fine aggregates in the lightweight concrete [17].

The numbers and dimensions of the specimens are shown in Table 1. The cross sections of the specimen were 120 mm × 50 mm and 200 mm × 70 mm, respectively. According to the Chinese specification GB50396-2014 [18], the specimens were designed with four width-thickness ratios, namely 40.00, 54.55, 66.67, and 90.91. The column slenderness ratios of 21.4 and 30.0 were in accordance with the requirements of the Chinese specimen GB50017-2017 [19]. The strengths of the inner lightweight concrete were LC20, LC25, and LC30, respectively. The dimensions of the specimens are shown in Figure 2; here, the specimens of Z200 series were taken as an example.

2.2. Material Properties. The compression strength of the various lightweight concretes was tested by standard cubic blocks. The blocks with dimension of 100 mm × 100 mm × 100 mm were made of the lightweight aggregate concrete. The concrete mixture ratio of LC20, LC25, and LC30 is shown in Table 2.

Three blocks were made for each strength grade. After maintaining for 24 hours, the molds were removed. Then, the compressive strength of the cube blocks was tested after 28 days [20]. The tested blocks are shown as Figure 3. The results are shown in Table 3. The average value of the three blocks was taken as the strength of the concrete.

2.3. Loading Scheme and Measurement Point Arrangement. The loading was carried out on an electro-hydraulic servo tester. To prevent the specimen from the foot type damage, the head plate was placed on the two ends of the specimen during the loading process, as shown in Figure 4. The loading was divided into two stages. The first step was preloading. A prepressure of 5 kN was applied to check whether the strain gauges, displacement gauges, and load channels were working properly. The second step was the formal loading. The displacement control was adopted, with each level loading by 0.5 mm. The loading was terminated when the load dropped to 70% of the ultimate load after the specimen was damaged.

The loading arrangement is shown in Figure 5. To measure the axial compression deformation of the specimen, the lateral displacement of the upper end, and the deflection in the middle of the specimen, axial displacement meters were arranged at the top of the specimen. Lateral displacement meters were arranged at the long and short sides, respectively, to measure the lateral displacement of the upper end of the specimen. Transverse displacement meters were also arranged in the middle height of the specimen at the long side and short side.

On the tube surface of the specimens, axial radial strain gauges were arranged at the upper and 1/4 height of the specimen as well as the middle position, respectively. The measurement points on the specimens of Z200 series are shown in Figure 6.

3. Experimental Phenomena and Data Analysis

3.1. Experimental Phenomena. During the loading, the damage process of the infilled concrete specimens was basically similar. At the beginning, only slight change appeared on the specimens. When close to the ultimate load, the bulge

(a) (b) (c)

Figure 1: Manufacturing process of the specimen. (a) Hollow built-up column. (b) Concrete pouring process. (c) Processed specimens.

Table 1: Parameters of the specimens.

No.	Cross section height (mm)	Component length (mm)	Component thickness (mm)	Concrete strength	Section width-to-thickness ratio	Steel pipe cross-sectional area (mm^2)	Steel content	Slenderness ratio
Z120-2.2-20	120	1500	2.2	LC20	54.55	932	15.5%	30
Z120-2.2-25	120	1500	2.2	LC25	54.55	932	15.5%	30
Z120-2.2-30	120	1500	2.2	LC30	54.55	932	15.5%	30
Z120-2.2-k	120	1500	2.2	Hollow	54.55	932	—	30
Z120-3.0-20	120	1500	3.0	LC20	40	1140	19%	30
Z120-3.0-25	120	1500	3.0	LC25	40	1140	19%	30
Z120-3.0-30	120	1500	3.0	LC30	40	1140	19%	30
Z120-3.0-k	120	1500	3.0	Hollow	40	114	—	30
Z200-2.2-20	200	1500	2.2	LC20	90.91	1188	8.5%	21.4
Z200-2.2-25	200	1500	2.2	LC25	90.91	1188	8.5%	21.4
Z200-2.2-30	200	1500	2.2	LC30	90.91	1188	8.5%	21.4
Z200-2.2-k	200	1500	2.2	Hollow	90.91	1188	—	21.4
Z200-3.0-20	200	1500	3.0	LC20	66.67	1620	11.6%	21.4
Z200-3.0-25	200	1500	3.0	LC25	66.67	1620	11.6%	21.4
Z200-3.0-30	200	1500	3.0	LC30	66.67	1620	11.6%	21.4
Z200-3.0-k	200	1500	3.0	Hollow	66.67	1620	—	21.4

appeared on the upper end of the steel tube near the restraint part. After that, the steel wall quickly bulged outward and the loading drops rapidly, as shown in Figure 7. The loading was terminated. After cutting the steel wall, it can be found that the concrete close to the buckling tube was crushed, and the rest surface was smooth, as shown in Figure 8. The specimens did not appear out-of-plane instability under loading, and the self-tapping screws were not dislodged.

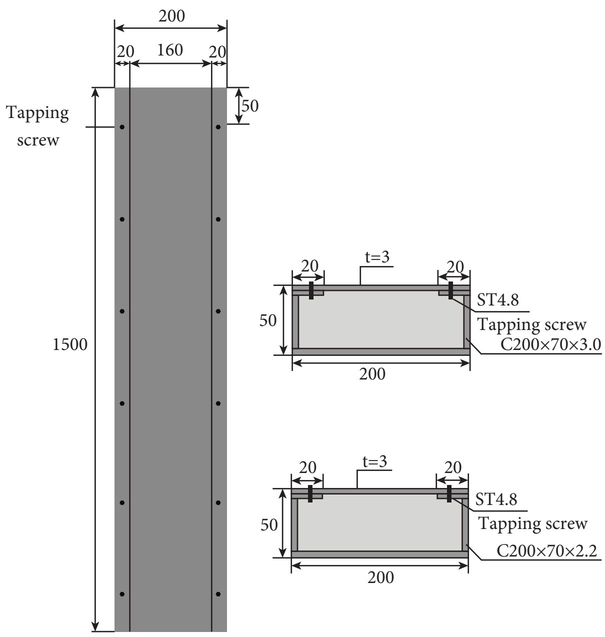

Figure 2: Dimensions of the specimen Z200 series (unit: mm).

Table 2: Mixture ratio of lightweight aggregate concrete (unit: kg/m^3).

Strength grade	Cement	Ceramsite	Expanded perlite	Water
LC20	380	838.8	50.76	200
LC25	420	838.8	50.76	200
LC30	460	838.8	50.76	200

Figure 3: Concrete blocks in the compressive strength test.

Table 3: Compressive strength of the lightweight concrete (unit: MPa).

Strength grade	LC20	LC25	LC30
Block No. 1	21.6	25.8	31.2
Block No. 2	20.3	26.7	33.5
Block No. 3	22.4	24.8	30.7
Average	21.4	25.8	31.8

Compared with the infilled concrete specimen, the buckling failure was more significant in the hollow specimen. At the beginning of loading, there is no obvious change on the appearance of the specimen. When the load was closed to the ultimate bearing capacity, the buckling at the end of the tube wall occurred. Then the loading drops rapidly. The buckling damage of the specimen is shown in Figure 9.

Figure 4: Head plate on the ends of specimens.

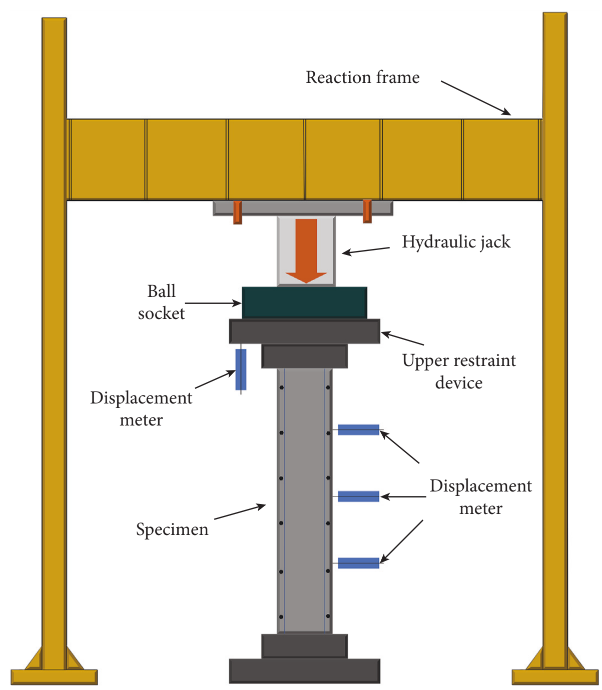

Figure 5: Loading diagram.

3.2. Relationship between Load and Displacement. The load-displacement curves of the infilled concrete specimen are shown in Figure 10. It can be found that the bearing capacity of the Z120 series specimens is smaller than that of the Z200 series under the same condition. The initial damage of the specimen generally occurred when the load reaches 70% of the ultimate bearing capacity.

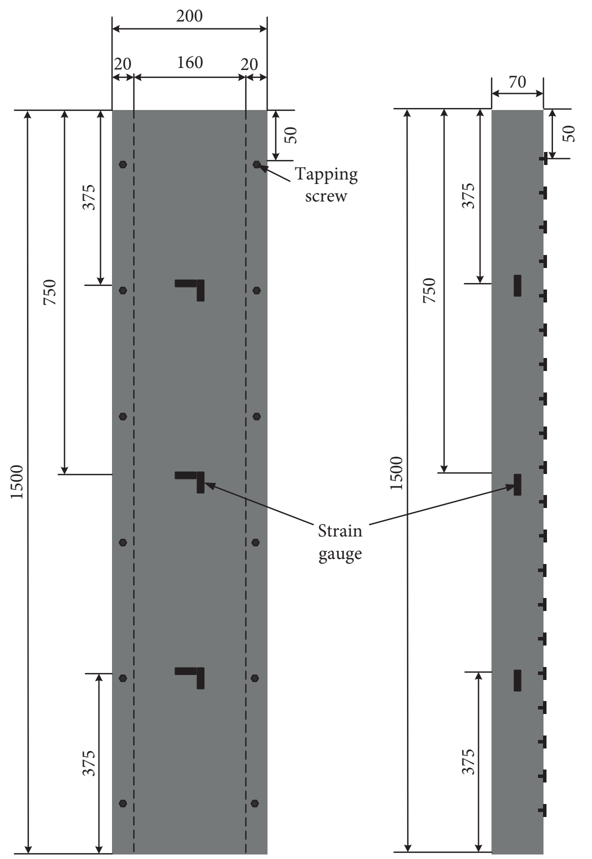

Figure 6: Layout of measuring points of Z200 series (unit: mm).

Figure 7: Local buckling damage.

Figure 8: Inner concrete crushed close to the buckling wall.

The arrangement of strain gauges on the cross section of the specimen is shown in Figure 11. Taking the load-strain curve of the cross section of the specimen Z200-2.2-25 as an example (as shown in Figure 12), the axial strains in the cross section were all negative, which indicated that the middle part of the specimen was under compression from the beginning of loading. The steel wall of *B* face and *C* face entered the yield state.

3.3. Effect of Steel Content on Ultimate Bearing Capacity and Ductility of the Specimen. Based on equation (1), the ductility coefficient was calculated to represent the ductility capacity of the members [21].

$$\mu = \frac{\varepsilon_{85\%}}{\varepsilon_u}, \quad (1)$$

where $\varepsilon_{85}\%$ is the average strain when the load drops to 85% of the ultimate bearing capacity of the specimen. ε_u is the average strain when the load reaches the ultimate bearing capacity of the specimen.

The bearing capacity and ductility coefficient of the specimens with the various concrete strength and steel contents were mainly compared, as shown in Tables 4 and 5. The corresponding slenderness ratio of steel content 8.5% and 11.6% is 21.4 and the rest is 30. It can be found that (1) the bearing capacity of the specimen increases with the strength of concrete. When the slenderness ratio is same, the bearing capacity of the specimens with higher steel content is larger than that of lower steel content. (2) In the same slenderness ratio, the ductility of the specimen with more steel content is better than that with lower steel content. Concrete strength has little influence on the ductility of the specimen.

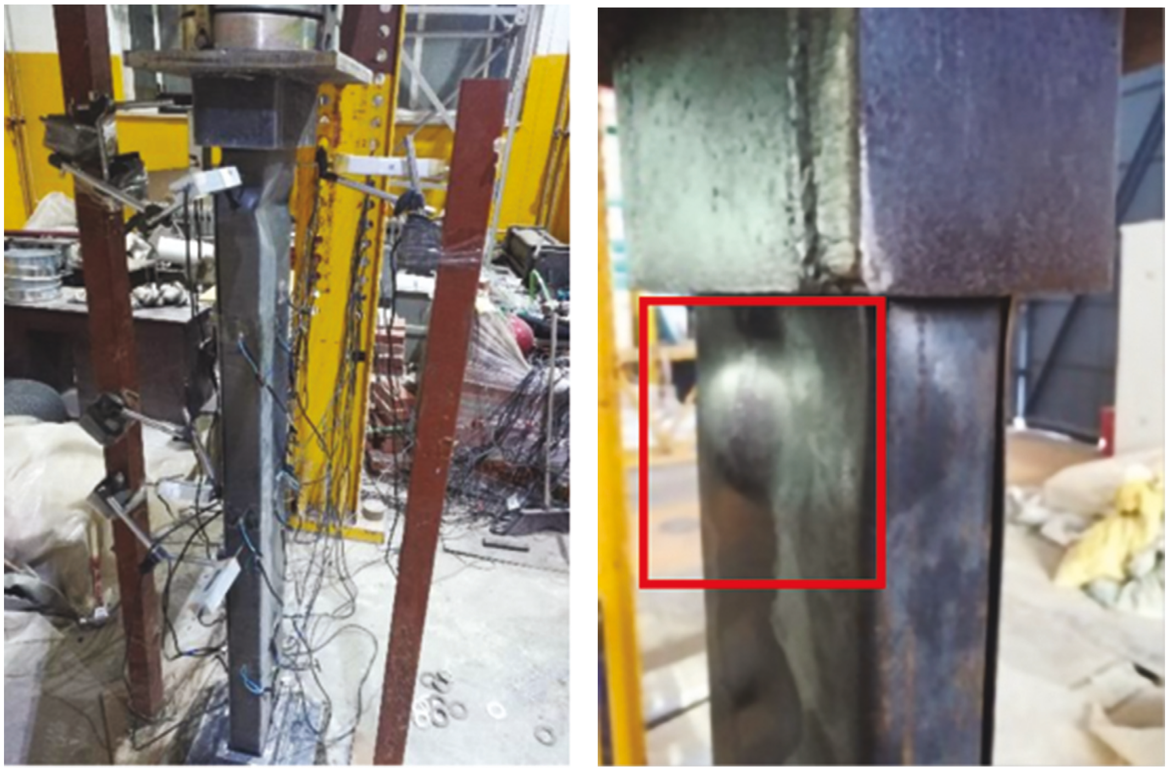

(a) (b)

Figure 9: Damage of the specimen Z200-3.0-k. (a) Overall. (b) Local buckling.

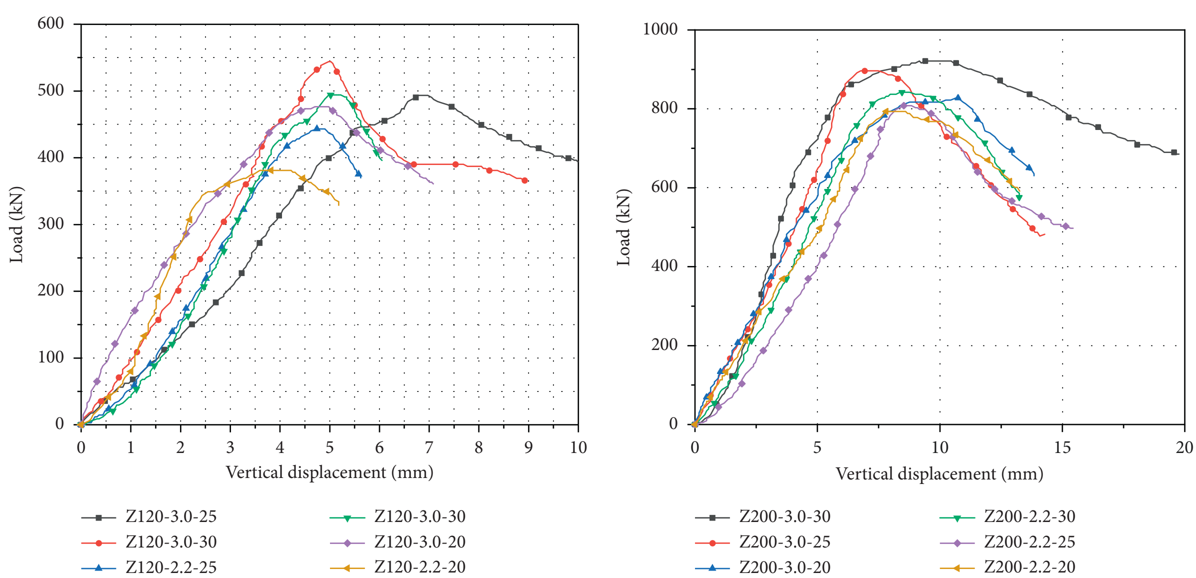

(a) (b)

Figure 10: Load-displacement curves. (a) Z120 series. (b) Z200 series.

4. Calculation Method of the Bearing Capacity

Referenced to the calculation method for the compressive bearing capacity of steel tube concrete from the specifications such as Japanese design and construction guidelines for steel tube concrete structures(AIJ-1997) [22], Chinese technical regulations for wartime military port rescue early strength combined structures (GJB4142-2000) [23], Fujian Provincial Standard Steel tube concrete structure technical regulations (DBJB-51-2003) [24], and technical specification

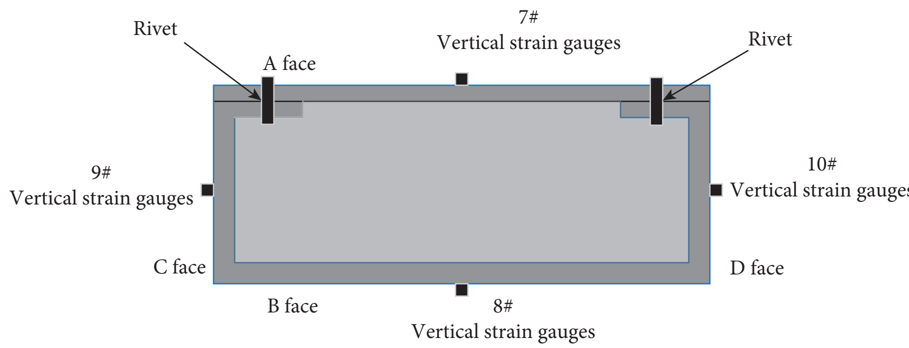

FIGURE 11: Arrangement of strain gauge on the section.

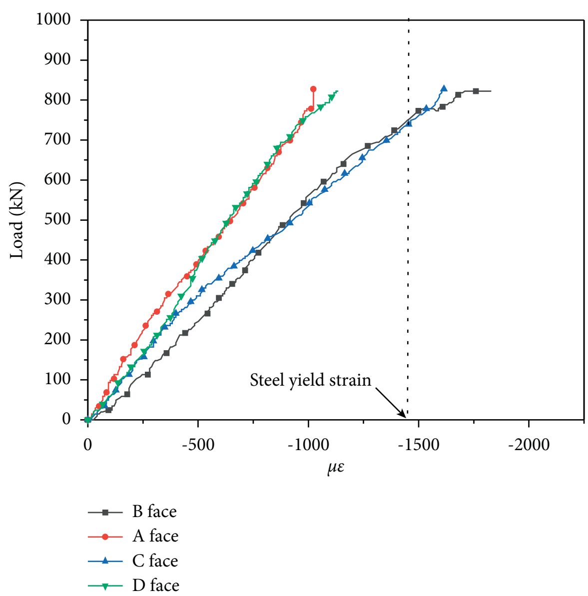

FIGURE 12: Load-strain curves of Z200-2.2-25.

TABLE 4: Ultimate bearing capacity with various percentages of steel content of specimens (unit: MPa).

Concrete strength	Steel content			
	8.5%	11.6%	15.5%	19%
LC20	810.40	849.32	392.36	497.88
LC25	832.41	929.05	453.23	511.99
LC30	848.93	935.18	499.22	540.83

TABLE 5: Ductility factor with various percentages of steel content of specimens.

Concrete strength	Steel content			
	8.5%	11.6%	15.5%	19%
LC20	1.44	1.54	1.01	1.12
LC25	1.46	1.58	1.14	1.14
LC30	1.55	1.60	1.21	1.15

for steel tube concrete structure (GB50936-2014) [18], the ultimate bearing capacity of the specimen in the test are compared with the design value. The results are shown in Table 6.

As can be found in Table 6, the ultimate bearing capacity of the specimens is greater than the design value of the existing codes. There is not a professional code to guide the design of cold-formed thin-walled steel tube concrete built-up members. Therefore, the calculation method of the ultimate bearing capacity of the members is proposed based on the superimposed strength theory of steel pipe concrete. The formula for calculating the compressive strength design value of the cold-formed thin-walled steel lightweight concrete member is presented in equation (2).

$$N_u = \varphi N_{0}, \tag{2}$$

$$N_0 = k_c f_c A_c + f_y A_s, \tag{3}$$

$$\xi = \alpha_{sc} \frac{f_y}{f_c}, \tag{4}$$

$$\varphi = \frac{1}{2\overline{\lambda}_{sc}^2}\left[\overline{\lambda}_{sc}^2 + \left(1 + 0.25\overline{\lambda}_{sc}\right) - \sqrt{\left(\overline{\lambda}_{sc}^2 + \left(1 + 0.25\overline{\lambda}_{sc}\right)\right)^2 - 4\overline{\lambda}_{sc}^2}\right], \tag{5}$$

$$\overline{\lambda}_{sc} = 0.01\lambda_{sc}\left(0.001 f_y + 0.45\right), \tag{6}$$

where k_c is the concrete strength correction coefficient related to the casing hoop steel coefficient ξ. f_y and f_c are the design values of steel and concrete strengths, respectively. A_c and A_s are the core concrete and steel tube cross-sectional areas. α_{sc} is the steel content of the member. φ is the stability factor of axial compression member. λ_{sc} and $\overline{\lambda}_{sc}$ are the slenderness ratio and normalized slenderness ratio of the members.

The regression analysis of k_c with ξ (as shown in Figure 13) was performed according to the test results to obtain the concrete strength reduction coefficient k_c, which is shown in the equation (7). Here, the correlation coefficient $R2$ is 0.82.

Table 6: Comparison of calculated bearing capacity of codes.

Specimen no.	Ultimate bearing capacity in test (kN)	Design bearing capacity/ultimate bearing capacity				
		AIJ-1997	GJB4142-2000	DBJB-51-2003	CECS159-2001	GB50936-2014
Z120-2.2-20	392.67	0.885	0.621	0.606	0.670	0.428
Z120-2.2-25	453.83	0.804	0.568	0.560	0.599	0.392
Z120-2.2-30	499.17	0.765	0.547	0.543	0.562	0.378
Z120-2.2-k.	291.67	0.959	—	—	—	—
Z120-3.0-20	503.50	0.809	0.553	0.549	0.621	0.380
Z120-3.0-25	514.81	0.823	0.565	0.568	0.623	0.388
Z120-3.0-30	556.67	0.790	0.548	0.556	0.591	0.377
Z120-3.0-k	403.17	0.848	—	—	—	—
Z200-2.2-20	819.00	0.645	0.483	0.459	0.529	0.218
Z200-2.2-25	838.83	0.681	0.516	0.494	0.547	0.235
Z200-2.2-30	855.01	0.719	0.552	0.531	0.567	0.254
Z200-2.2-k	316.00	1.128	—	—	—	—
Z200-3.0-20	843.33	0.773	0.563	0.540	0.646	0.253
Z200-3.0-25	916.00	0.757	0.557	0.539	0.622	0.253
Z200-3.0-30	936.67	0.785	0.585	0.569	0.635	0.268
Z200-3.0-k	436.10	1.114	—	—	—	—

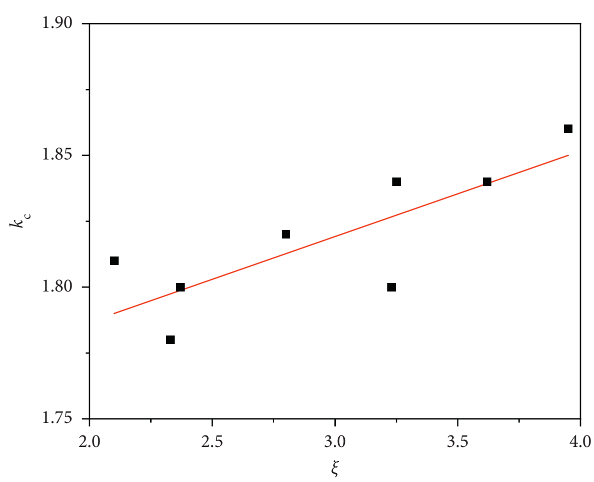

Figure 13: Regression curve of k_c and ξ.

Table 7: Comparison of calculated and test values.

Specimen no.	ξ	k_c	N_u	N	N/N_u
Z120-2.2-20	3.47	1.41	411.67	392.67	0.95
Z120-2.2-25	2.80	1.74	437.84	453.83	1.04
Z120-2.2-30	2.33	1.83	463.56	499.17	1.08
Z120-3.0-20	4.26	2.10	474.17	503.50	1.06
Z120-3.0-25	3.43	1.80	499.33	514.81	1.03
Z120-3.0-30	2.86	1.86	524.00	556.67	1.06
Z200-2.2-20	1.90	2.29	691.32	819.00	1.18
Z200-2.2-25	1.54	1.91	737.19	838.83	1.14
Z200-2.2-30	1.28	1.64	803.42	855.01	1.06
Z200-3.0-20	2.60	1.83	805.88	843.33	1.05
Z200-3.0-25	2.10	1.76	870.67	916.00	1.05
Z200-3.0-30	1.74	1.54	934.55	936.67	1.00

$$k_c = 0.1696\xi + 1.3643. \quad (7)$$

Therefore, equation (8) is used to calculate the compressive bearing capacity of the member.

$$N_o = (0.1696\xi 1.3643) f_c A_c f_y A_s \quad (8)$$

The comparison of the ultimate bearing capacity N_u is obtained based on equation (2) and the test results N is shown in Table 7.

As can be found from Table 7, N_u/N ranged from 0.95 to 1.18, with a mean value of 1.06. The standard deviation is 0.06 and the variation coefficient is 0.05, which indicate that the equation results are in good agreement with the experimental values.

5. Finite Element Analysis

5.1. Construction of Finite Element Model. To explore the finite element analysis method, the cold-formed thin-walled steel lightweight concrete built-up column was analyzed in ABAQUS. The steel tube was meshed by the four nodes curved shell element (S4R) with the Simpson integration rule. The inner concrete was simulated by three-dimensional solid element (C3D8R) in eight-node hexahedral linear reduced integral format. The element size was about 20 mm. The meshed model is shown as Figure 14.

The damaged plasticity model and the simplified elastic-plastic model satisfied the V. The Mises yield criterion was used to simulate the material performance of the concrete and steel. The hard contact was set to simulate the contact between the steel tube and the infilled concrete in normal direction, and the bonded slip was set in the tangential direction.

5.2. Verification of Finite Element Analysis Results. The FEM models of the specimen in the test were constructed and analyzed. Here, we have taken specimens Z120-2.2-20 and Z200-2.2-20 as examples to demonstrate the damage results, as shown in Figures 15 and 16. It can be found that the damage state of the FEM model is consistent with the test. Both of them are the local buckling of the steel tube. And the inner concrete was crushed at the bucking location of the tube and the rest was still intact which was consistent with the damage phenomenon of the opened specimen after the test, as shown in Figure 17.

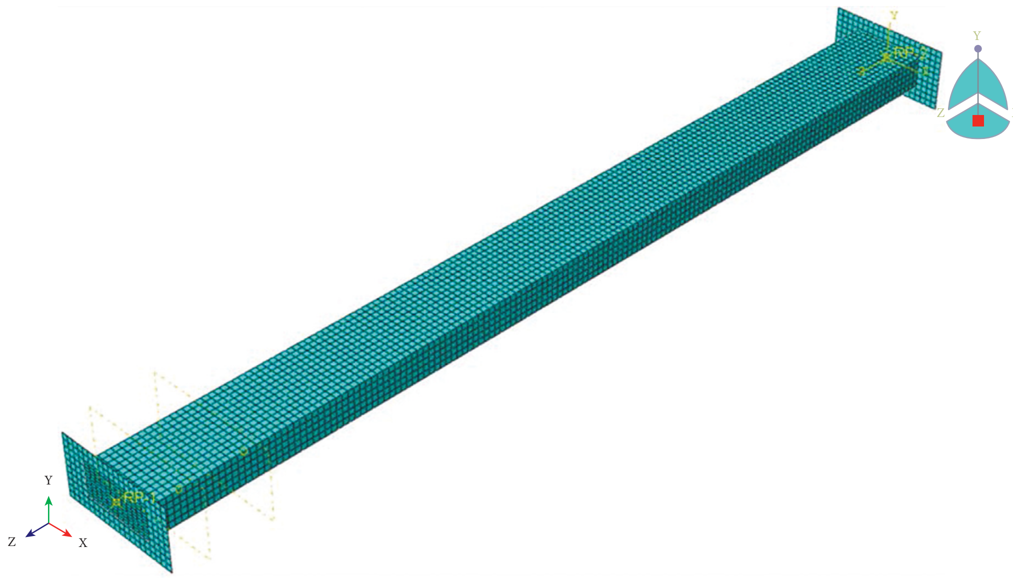

Figure 14: FEM model of the cold-formed thin-walled steel light-weight concrete built-up column.

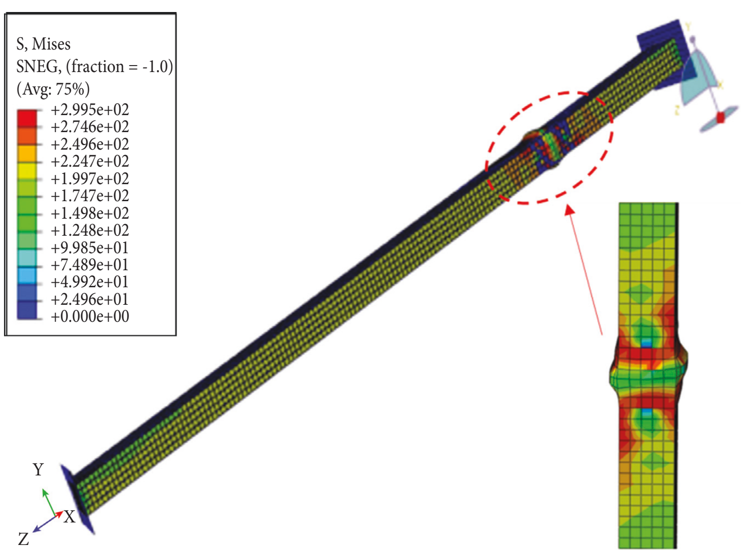

(a)

(b)

Figure 15: Result comparison of FEM and test for the specimen Z120-2.2-20. (a) FEM result. (b) Test damage.

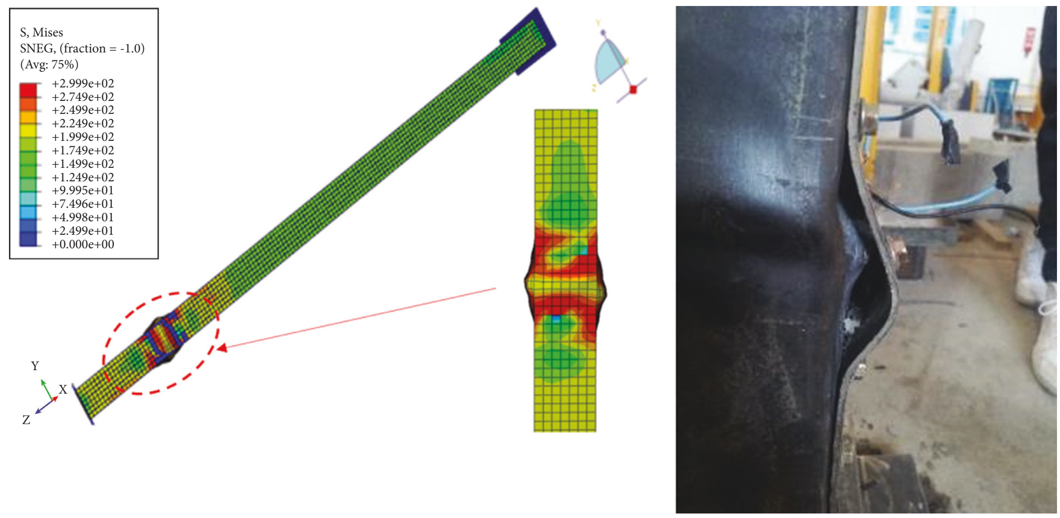

(a) (b)

Figure 16: Result comparison of FEM and test for the specimen Z200-2.2-20. (a) FEM result. (b) Test damage.

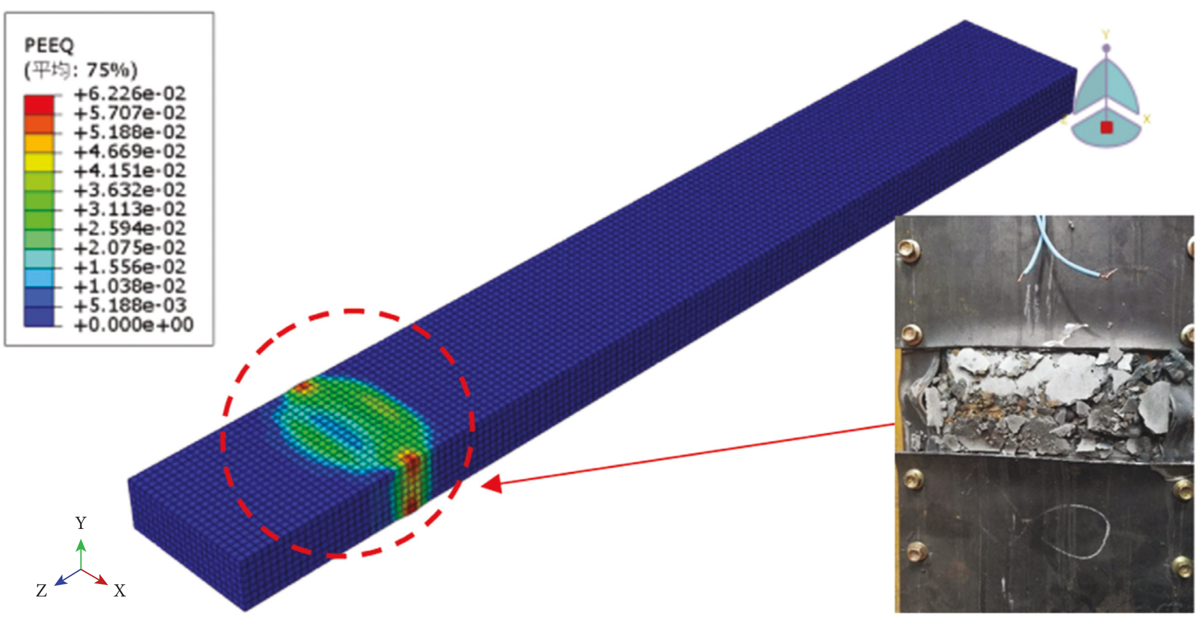

Figure 17: Equivalent plastic strain cloud of core concrete in the specimen Z2000-2.2-20.

Table 8: Comparison of ultimate bearing capacity.

Specimen no	FEM results $N1$ (kN)	Test results $N2$ (kN)	$N1/N2$
Z120-2.2-20	364.96	392.67	0.93
Z120-3.0-20	444.66	503.50	0.88
Z120-2.2-25	420.44	453.83	0.93
Z120-3.0-25	453.22	514.81	0.88
Z120-2.2-30	445.01	499.17	0.89
Z120-3.0-30	508.98	556.67	0.91
Z200-2.2-20	754.63	819.00	0.92
Z200-3.0-20	767.00	843.33	0.91
Z120-2.2-25	760.77	838.83	0.91
Z120-3.0-25	850.67	916.00	0.93
Z120-2.2-30	779.79	855.01	0.91
Z120-3.0-30	835.48	936.67	0.89

The ultimate bearing capacity of the FEM model and the test are compared in Table 8. It can be found that the average value of the ratios is 0.88. The difference is less than 15%. The analysis method can represent the interaction between the steel tube and concrete.

6. Conclusion

(1) The main failure mode of the cold-formed thin-walled steel lightweight concrete built-up column is the local buckling of steel tube wall and partially crushed of the internal concrete. Due to the lack of internal concrete restraint, the hollow members showed earlier local buckling of the steel wall and

lower load capacity compared to the infilled concrete members

(2) The bearing capacity of cold-formed thin-walled steel lightweight concrete built-up columns increases with the strength of the infilled concrete. In the same slenderness ratio, the bearing capacity and ductility of the members with more steel content are higher than those of lower steel content

(3) Based on the material superimposed strength theory, the calculation method of bearing capacity for the cold-formed thin-walled steel lightweight concrete built-up column is proposed, which is verified by comparing with the experimental results

Data Availability

The experimental data used to support the findings of this study are included within the article.

Conflicts of Interest

The authors declare that there are no conflicts of interest regarding the publication of this paper.

Acknowledgments

This work was financially supported by the National Natural Science Foundation of China (grant nos. 51408009 and 51608010), Fundamental Research Funds for the Beijing's Universities (110052971921/062), and Yuyou Talent Project of North China University of Technology (grant no. XN012/044) for this study.

References

[1] X. J. Gao, J. Q. Yu, and M. Z. Lin, "Application of cold-formed steel in light steel construction," *New Building Materials*, vol. 4, pp. 8–177, 1999.

[2] Y. P. Song, *Constitutive Relations and Failure Criteria of Various concrete Materials*, China Water Power Press, Beijing, China, 2002.

[3] Y. H. Yao and Z. Y. Wu, "Effects of distortional imperfections on mechanical properties of cold-formed thin-walled steel columns," *Journal of Shenzhen University*, vol. 29, no. 5, pp. 421–426, 2012.

[4] J. Whittle and C. Ramseyer, "Buckling capacities of axially loaded, cold-formed, built-up C-channels," *Thin-Walled Structures*, vol. 47, no. 2, pp. 190–201, 2009.

[5] T. H. Zhou and D. H. Yang, "Experimental study and numerical analysis on axial compression performance of cold-formed thin-walled steel section columns with four limbs," *China Civil Engineering Journal*, vol. 45, no. 1, pp. 77–85, 2012.

[6] Y. Li, M. Jim, and J. G. Xiong, "Experimental study on the axial compressive bearing capacity of thin-walled concrete-filled steel tube columns," *Concrete*, vol. 11, pp. 47–49, 2008.

[7] S. F. Nie and Y. Y. Huo, "Experimental research and numerical analysis on the eccentric stress performance of cold-formed thin-walled steel four-legged box columns," *China Civil Engineering Journal*, vol. 49, no. 10, pp. 1–10, 2016.

[8] S. F. Nie and T. H. Zhou, "Compression test research and finite element analysis of double-limb cold-formed thin-walled steel box columns," *Journal of Building Structures*, vol. 38, no. 10, pp. 10–20, 2017.

[9] X. H. Zhou and Y. Guan, "Research on bending performance of double-limb combined cold-formed thin-walled steel I-section beam," *China Civil Engineering Journal*, vol. 49, no. 8, pp. 16–27, 2016.

[10] C. D. Moen and B. W. Schafer, "Experiments on cold-formed steel columns with holes," *Thin-Walled Structures*, vol. 46, no. 10, pp. 1164–1182, 2008.

[11] J. S. Chen, *Experimental Study and Theoretical Analysis of Flexural Performance of Lightweight Aggregate concrete Filled Steel Tubes*, Hehai University, Jiangsu, China, 2007.

[12] B. Young and J. Chen, "Design of cold-formed steel built-up closed sections with intermediate stiffeners," *Journal of Structural Engineering*, vol. 134, no. 5, pp. 727–737, 2008.

[13] B. Uy, "Local and post local buckling of concrete filled steel welded box columns," *Journal of Constructional Steel Research*, vol. 47, no. 1-2, pp. 47–72, 1998.

[14] M. D. Pircher, M. D. O' Shea, and R. Q. Bridge, "The influence of the fabrication process on the buckling of thin-walled steel box sections," *Thin-Walled Structures*, vol. 40, no. 2, pp. 109–123, 2002.

[15] Y. F. An and L. H. Han, "Behaviour of concrete-encased CFST columns under combined compression and bending," *Journal of Constructional Steel Research*, vol. 101, pp. 314–330, 2014.

[16] L. H. Han, C. C. Hou, X. L. Zhao, and K. J. Rasmussen, "Behaviour of high-strength concrete filled steel tubes under transverse impact loading," *Journal of Constructional Steel Research*, vol. 92, pp. 25–39, 2014.

[17] W. Ding, L. S. Gong, and Y. C. Zhou, *Technical Specification for Lightweight Aggregate Concrete*, Ministry of Construction of the People's Republic of China, China, 2002.

[18] X. X. Zha, C. Z. Xiao, and S. T. Zhong, *Technical Code for concrete-filled Steel Tube Structure*, Ministry of Housing and Urban Rural Development of the People's Republic of China, China, 2014.

[19] S. Shi, L. J. Wang, and H. Q. Yu, *Design Code for Steel Structure*, Ministry of Housing and Urban Rural Development of the People's Republic of China, china, 2017.

[20] H. B. Ge and T. Usami, "Strength of concrete-filled thin-walled steel box columns: experiment," *Journal of Structural Engineering*, vol. 118, no. 11, pp. 3036–3054, 1992.

[21] J. Yang, *Research on the Axial Compression Performance of Steel Tube-Recycled concrete Short Columns*, Huaqiao University, Quanzhou, China, 2012.

[22] Architectural Institute of Japan, *Recommendations for Design and Construction of concrete Filled Steel Tubular Structures*, Architectural Institute of Japan, Tokyo, Japan, 1997.

[23] Z. Wei, L. Han, X. L. Liu, and S. Y. Zhang, *Wartime Military Port Emergency Repair Early-Strength Combined Structure Technical Regulations*, The General Logistics Department of the Chinese People's Liberation Army, Beijing, China, 2000.

[24] Z. Tao, H. Chen, and Q. Yu, *Technical Specification for Steel Tube concrete Structure*, Department of Housing Construction of Fujian Province, Fujian, Taiwan, 2003.